THE JOURNAL OF PHYSICAL CHEMISTRY C

Article

Cite This: J. Phys. Chem. C 2018, 122, 20083−20089

pubs.acs.org/JPCC

Surface Plasmon Polariton-Controlled Molecular Switch

Alexandre Giguère,[†,‡] Matthias Ernzerhof,[*,†] and Didier Mayou[§]

[†]Département de Chimie, Université de Montréal, C.P. 6128, Succursale A, Montréal, Québec H3C 3J7, Canada

[‡]Département des Sciences de la Nature, Collège Militaire Royal de Saint-Jean, Saint-Jean-sur-Richelieu, Québec J3B 8R8, Canada

[§]Institut Néel, 25 Avenue des Martyrs, BP 166, Grenoble Cedex 9 38042, France

ABSTRACT: Molecular electronic devices are studied extensively to explore their potential use in electronics and also to gain an understanding of the mechanisms of electron transport at the molecular scale. Recent experiments show that molecules can be strongly coupled to surface plasmon polaritons (SPPs) and that the resulting, the so-called, dressed molecular states are the entanglements of electrons and SPPs. Here, we propose molecular electronic devices that are derived from dressed molecules. We present a simple, analytical theory that shows how SPPs can provide a complete control of the molecular conductance. In a suggested device, the SPP couples a localized excited state to the continuum wave function of the molecular conductor, and the details of this coupling, that is, frequency and field strength of the SPP, are the parameters that modulate the molecular conductance. In addition to the molecular switch, we also design a photovoltaic cell that harvests the SPP energy to generate a photocurrent. The proposed SPP-controlled devices represent a novel type of optoelectronic circuitry that significantly enlarges the potential of molecular electronics.

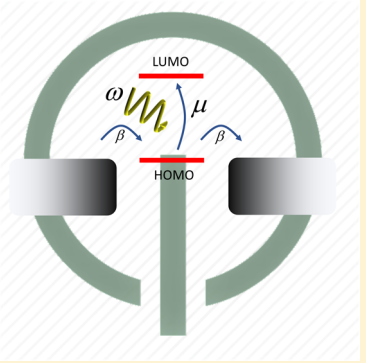

Downloaded via NORTHWESTERN UNIV on July 18, 2025 at 03:59:47 (UTC).
See https://pubs.acs.org/sharingguidelines for options on how to legitimately share published articles.

1. MIXED STATES OF MATTER AND LIGHT

Photons or surface plasmon polaritons (SPPs) that interact strongly with molecules produce mixed states of matter and light, exhibiting intriguing and often uncharted properties.[1] We focus on one particular aspect of these matter−light systems, namely, their electron conductance.[2,3] Molecular electronic devices (MEDs) have been receiving considerable interest,[4,5] and numerous MEDs have been proposed and realized experimentally. One particular class of MEDs exploits the wave function interference[6−9] to control the molecular conductance, an example is provided by the side-chain effect proposed in refs[7,10] and verified experimentally in, for example, refs[11−15] The side-chain effect uses the localized states of the MED to suppress the conductance: for a certain energy, the localized and the continuum states interfere to prevent the device wave function from extending over the two external contacts. One device proposed here, an SPP-operated switch, represents a transcription of the side-chain effect to the realm of the mixed matter−light states. Its underlying molecule features a localized excited state which is coupled to the continuum states through the SPP, allowing for the complete suppression of the conductance.

A motivation for proposing the SPP-operated switch is provided by the recent reports of experiments where molecules are strongly coupled to SPPs.[16−19] In these experiments, the molecule is placed between two gold surfaces that sustain the SPP. As the molecule can be chemically bonded to the contacts,[17] the application of a voltage between both gold electrodes should allow for the measurement of the conductance through the SPP−molecule system. An arrangement that we envision to study the SPP−molecule coupling is depicted in Figure 1, which resembles the ones used in refs.[16,17] The transmission probability $T(E)$ of the device, which is proportional to its conductance $g(E)$, $g(E) = \frac{2e^2}{h}T(E)$, is plotted in panel (b) of Figure 1 against the energy of the traversing electron. $T(E)$ is obtained employing the theory detailed below (section 2), using a Hückel Hamiltonian for the description of the molecule. The molecule−SPP coupling results in the complete suppression of the conductance through the device at the energy (ϵ_{HOMO}) of the highest occupied molecular orbital (HOMO) of azulene, that is, $T(\epsilon_{\mathrm{HOMO}}) = 0$. For the molecule−SPP system at resonance, the HOMO interacts strongly with the localized, lowest unoccupied molecular orbital (LUMO). Without the molecule−SPP coupling, the HOMO creates a maximum in the transmission probability with $T(\epsilon_{\mathrm{HOMO}}) = 1$. As in the case of the side-chain effect of molecular electronics, the proposed mechanism should be observable and should provide a stepping stone for SPP-controlled electronics. In section 2, we develop an analytical model for an SPP-controlled molecular conductor and show how the parameters of the SPP, namely frequency and field strength, control the conductance through the molecule. Sophisticated theories are now available[20−22] for the description of mixed photon−electron systems; however, these approaches are not readily amenable to a simple, transparent paper-and-pencil treatment that we opt for here. Our theory, which treats the SPP field as a quantized field, follows earlier works[23,24] in which the interaction of light with molecular conductors is also described in terms of a quantized photon field interacting with two-level electronic systems.

Received: May 30, 2018
Revised: August 2, 2018
Published: August 10, 2018

© 2018 American Chemical Society

DOI: 10.1021/acs.jpcc.8b05190
J. Phys. Chem. C 2018, 122, 20083−20089

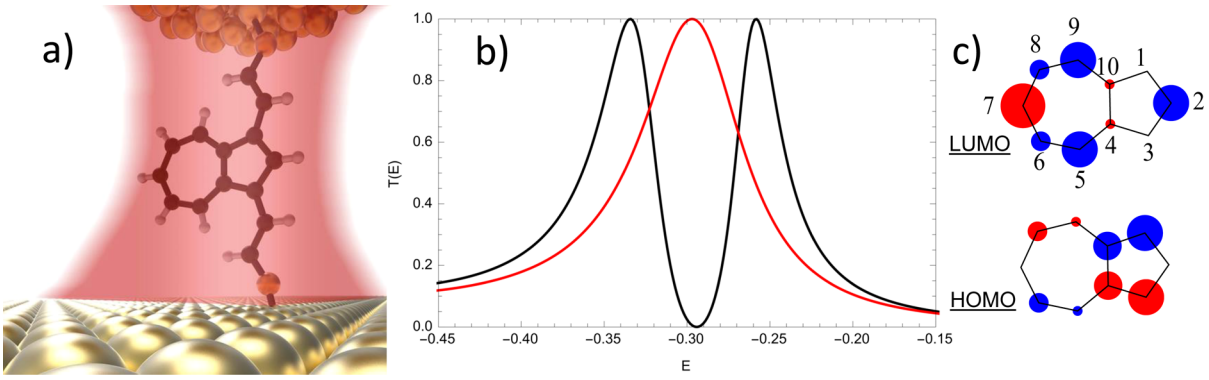

Figure 1. Example of an SPP-controlled molecular switch. The structure of the switch is shown in panel (a) where 1,3-divinylthioazulene couples strongly to the SPP that is sustained by the gold structure, resulting in dressed molecular states. Simultaneously, 1,3-divinylthioazulene is chemically bonded to gold surfaces through sulfur bridges. Variation in the SPP parameters, that is, its field strength and frequency, allows for a complete control of the molecular conductance. In panel (b), the transmission probability $T(E)$ of the device is plotted as a function of the energy of the traversing electron. For the SPP−molecule system at resonance (black curve), $T(E)$ vanishes at the HOMO energy ($T(\epsilon_{\mathrm{HOMO}} = -0.295) = 0$), and the width of the gap in $T(E)$ is given by the Rabi frequency. For comparison, the red curve shows the transmission probability in the absence of the SPP. Arbitrary energy units are used; the peak positions, their widths, and separations are determined by the size of the various coupling parameters in the system; a detailed discussion is provided in section 2. The HOMO and LUMO of the azulene molecule, as obtained from the Hückel Hamiltonian, are shown in panel (c). Connecting the contacts to atoms 1 and 3 of the azulene molecule will ensure that for an energy equal to that of the azulene LUMO, the wave function of a device will feature a molecule decoupled from the contacts. This localized state is a prerequisite for the SPP-induced conductance suppression. Note that the HOMO also has (axial) atoms with vanishing orbital coefficients; this feature is exploited in the molecular photovoltaic cell described in section 3.

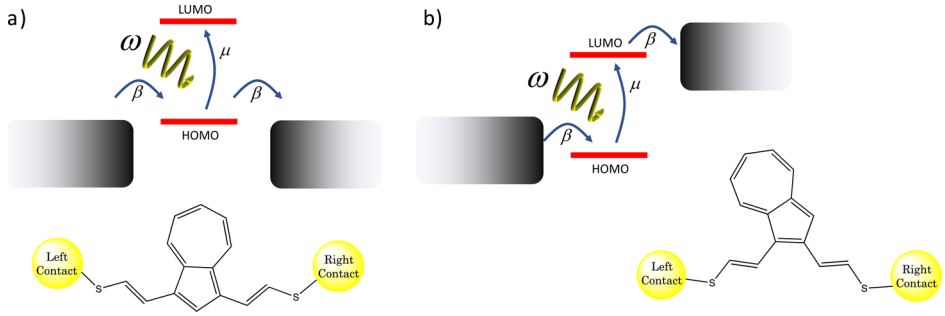

Figure 2. Electron transport mechanisms through strongly coupled molecule−SPP systems. (a) Two-level (HOMO and LUMO) system strongly interacting with an SPP giving rise to a HOMO−LUMO transition matrix element μ. μ is proportional to the electric field **E** times the transition dipole moment **d**. The resulting dressed molecule is coupled to the external contacts through the hopping parameter β. The energy quantum of the SPP is given by ω, which reduces the effective spacing between the HOMO and LUMO. The SPP couples a localized state (LUMO) to a continuum, resulting in a Fano resonance. The illustrated mechanism can, for instance, be realized by the device sketched below the scheme where azulene is connected such that its LUMO is isolated from the contacts; this is the configuration considered in Figure 1. (b) Mechanism of a photovoltaic cell, harvesting the SPP energy to generate a photoelectric current. The HOMO and LUMO are connected to the left contact (valence band) or right contact (conduction band), respectively. As a consequence, in the absence of SPPs, the conductance vanishes. The electron transport through the junction requires SPP quanta absorption and energy conversion. The asymmetric coupling of the orbitals to the contacts implies that the SPP quanta absorption results in a left-to-right current through the junction. The device below the scheme shows how to exploit the structure of the HOMO and LUMO of azulene, as depicted in Figure 1, to realize the asymmetric orbital−contact coupling.

The theoretical model that we propose here can be viewed as a generalization of the Jaynes−Cummings (JC) model,[25] which is fundamental to the theory of strong photon−atom interaction. To the JC model, we add the interaction of the molecule with external contacts, which results in a nontrivial model for SPP-controlled molecular electronics. In addition to the SPP control of the molecular conductance, the model that we present can also be employed to describe an inelastic process in which the SPP energy is absorbed and converted into an electronic excitation. This mechanism, described in detail in section 3, represents another JC-model extension for a coherent photovoltaic cell[26−28] that is strongly coupled to a photon source. Again, with the presently available experimental techniques, such a coherent molecular photocell should be within reach. Similar photovoltaic cells have been discussed in refs,[23,24] where abstract multilevel systems are considered; here, we add to this work by considering strong electromagnetic fields and by providing suggestions on how to exploit the molecular orbital structure to design such photovoltaic cells.

2. SPP-OPERATED SWITCH (ELASTIC SPP−MOLECULE INTERACTION)

The mechanism of an SPP-operated switch is explained using the scheme in Figure 2. We consider a molecule that features a localized excitation into the LUMO. The SPP electric field (**E**) in the junction couples to the transition dipole moment (**d**) of the HOMO−LUMO excitation of the molecule. The resulting HOMO−LUMO coupling matrix element is $\mu = -\mathbf{E}\mathbf{d}$. If the Rabi frequency (given by $2|\mu|$) is larger than the molecule−contact hopping frequency β, the electron passes numerous

DOI: 10.1021/acs.jpcc.8b05190
J. Phys. Chem. C 2018, 122, 20083−20089

times between the HOMO and the LUMO before it jumps off the molecule into a contact. This ensures that mixed states of light and matter are formed. We stress that only the HOMO is coupled to the external reservoirs, whereas the LUMO is assumed to be isolated from them. This might appear to be a rather artificial constraint, but there is an abundance of molecules with a LUMO that vanishes on various atoms, and connecting the contacts to these atoms results in an isolated excited state (cf. Figure 1).

The device sketched in panel (a) of Figure 2 is represented by a simple Hamiltonian matrix $\mathbf{H}$ (for a detailed discussion, we refer to ref 26)

$$\mathbf{H} = \begin{pmatrix} \delta & \mu \\ \mu & \dfrac{\mathrm{i}(r+1)\beta}{1-r} - \mathrm{i}\beta + \epsilon_{\mathrm{HOMO}} \end{pmatrix} \tag{1}$$

where $\frac{\mathrm{i}(r+1)\beta}{1-r}$ is the source potential[7,29] representing the left contact in the wide-band limit (WBL) and $-\mathrm{i}\beta$ is the sink potential representing the right contact in the WBL. The complex-valued source and sink potentials are the mathematical tools that generate and absorb electron current density, respectively. They replace the external reservoirs in a rigorous way and turn $\mathbf{H}$ into a function of the reflection coefficient r appearing in the source potential, that is, $\mathbf{H} = \mathbf{H}(r)$. δ is the effective energy of the excited state and is given by the actual value of the LUMO energy (ϵ_{LUMO}) shifted by the SPP frequency, that is, $\delta = \epsilon_{\mathrm{LUMO}} - \omega$. Therefore, the interaction of the molecule with the SPP reduces the HOMO−LUMO separation. The energy of the HOMO (ϵ_{HOMO}) is assumed to be equal to the Fermi energy of the leads, which in turn is set to zero, that is, $\epsilon_{\mathrm{HOMO}} = E_{\mathrm{F}} = 0$. Our model accounts for the electron degrees of freedom explicitly, and the SPP degrees of freedom have been integrated out;[26] they give rise to the parameters μ and δ in the Hamilton matrix of eq 1. When the electron is in the HOMO, there is an additional SPP quantum of energy in the system compared to the configuration in which the electron is in the LUMO. This additional energy quantum reduces the HOMO−LUMO gap by ω. In our model, one absorbed SPP quantum yields one excited electron. The field strength $|\mathbf{E}|$ is proportional to the square root of the number of SPP quanta,[26] and we suppose this number to be large, so that $|\mathbf{E}|$ remains constant upon SPP quanta absorption.

The quantity of interest is $T(E)$, which can be obtained through the solution of the secular equation for a given energy E

$$\det(\mathbf{H}(r) - E) = 0 \tag{2}$$

The unknown in this equation is the reflection coefficient r, which is determined, and the transmission probability is obtained according to $T(E) = 1 - |r(E)|^2$

$$T(E) = \frac{4\beta^2(\delta - E)^2}{4\beta^2(\delta - E)^2 + (E(\delta - E) + \mu^2)^2} \tag{3}$$

This expression contains various parameters which characterize a particular physical system. We examine the dependence of $T(E)$ on E, δ, and μ in detail; the latter two parameters characterize the SPP. As already mentioned, $|\mu|$ has to be of the order of $|\beta|$, or larger, for the formation of dressed states, meaning that the SPP-induced coupling of the molecular states has to be similar to or larger than the coupling of the molecular states to the contacts. In recent experiments, $|\mu|$ is on the order of a fraction of an electron volt, and, through the introduction of spacer groups between the molecule and the gold contacts, the molecule−contact coupling β can be reduced below that value. In the illustrations of $T(E)$, we arbitrarily set $\beta = 0.1$ and study $T(E)$ upon variation of the remaining parameters. A plot of $T(E)$ is shown in Figure 3. The various curves, obtained upon

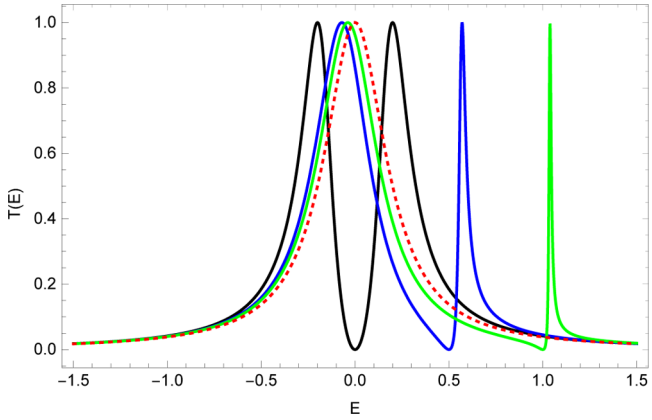

Figure 3. Transmission probability as a function of the electron energy. The various curves are obtained with different values of the shifted SPP frequency $\delta = \epsilon_{\mathrm{LUMO}} - \omega = 0$, 0.5, 1, yielding the black, blue, and green curves, respectively. The dotted transmission probability curve is obtained for the vanishing coupling between the SPP and the molecule; it shows a resonance in $T(E)$ at the HOMO energy. The molecule−contact coupling is arbitrarily set to $\beta = 0.1$ and $\mu = 0.2$.

variation of the SPP frequency, exhibit the typical Fano lineshape.[18,30,31] The Fano resonance is indicative of a localized state that couples to a continuum. The energy of the localized state (δ) is the energy at which the dressed molecule becomes insulating, that is, the electrons of energy δ cannot pass through the dressed molecule ($T(\delta) = 0$). As $\delta = \epsilon_{\mathrm{LUMO}} - \omega$, the suppression of the conductance is controlled through the SPP frequency ω. To ensure conductance suppression at E_{F}, the combined molecular−SPP system has to be at resonance, meaning that $\delta = 0$. In conventional molecular conductors, one expects a conductance maximum at the energy of the HOMO; however, in the dressed molecular conductor considered here, the conductance at the HOMO energy can be completely suppressed through the coupling of the molecule to the SPP. The various parameters in eq 3 characterize the specific form of the Fano resonance. We already discussed the role of δ; the effect of varying μ on the transmission probability is studied for the transmission probability at the Fermi energy $T(E)$, and at resonance $\delta = 0$, where we find that the two maxima in $T(E)$ are separated by the Rabi frequency $2|\mu|$ (see Figure 4). The remaining parameter β in eq 3, describing the coupling to the contacts, determines the width of the peaks in $T(E)$. For increasing $|\beta|$, the transmission probability approaches 1.

To better understand the features of the plots in Figures 3 and 4, we note that for $\beta = 0$ the eigenvalues of $\mathbf{H}$ in eq 1 are given by

$$\epsilon_1 = \frac{1}{2}(\delta - \sqrt{\delta^2 + 4\mu^2}), \qquad \epsilon_2 = \frac{1}{2}(\delta + \sqrt{\delta^2 + 4\mu^2})$$

which are the energies of the dressed states of the JC model, and they correspond to the energies of the maxima in both figures. This underscores the relation of our model for conductance to the JC model.

The discussion above assumes that the LUMO is isolated from the rest of the system. This point requires consideration, as in actual experiments there will most likely be some coupling of

DOI: 10.1021/acs.jpcc.8b05190
J. Phys. Chem. C 2018, 122, 20083−20089

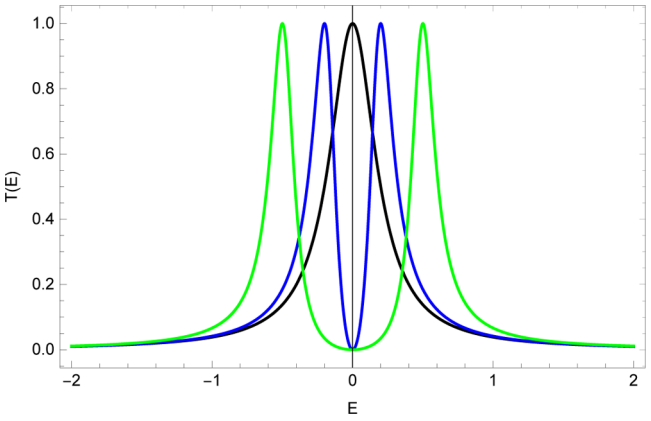

Figure 4. Transmission probability as a function of the electron energy. The dressed molecule is at resonance ($\delta = 0$) and the various curves are obtained for different values of the Rabi frequency ($=2|\mu|$) with $\mu = 0$, 0.2, 0.5, yielding the black, blue, and green curves, respectively. The width of the gap in the transmission probability is proportional to the Rabi frequency. The molecule−contact coupling is arbitrarily set to $\beta = 0.1$.

the LUMO to the leads or to another part of the system. To model this effect, we assign a finite lifetime to the LUMO. The lifetime is inversely proportional to the imaginary part of the energy ($-i\alpha$) that we add to δ in the matrix Hamiltonian of eq 1. Now, the transmission probability encompasses currents that leak out through the LUMO. Assuming that the electron that escapes from the LUMO is transferred into the right or the left lead, this process augments or reduces, respectively, the electron transport across the system. The leakage of the LUMO involves the absorption of a quantum from the SPP field and its conversion into electron energy. This process is the focus of another mechanism of the dressed molecular conductor which is discussed in section 3. The finite lifetime of the LUMO has an adverse effect on the device mechanism. To see this, we consider the $T(E)$ at the Fermi energy for an SPP frequency that corresponds to a resonance

$$T(0) = \frac{4\alpha\beta(\alpha\beta + \mu^2)}{(2\alpha\beta + \mu^2)^2} = \frac{4\alpha\beta}{\mu^2} + O(\alpha^2) \tag{4}$$

As shown above, for $\alpha = 0$, we find $T(0) = 0$. In case where $\alpha > 0$, $T(0)$ increases, and the current suppression through the SPP diminishes. For small values of α, $T(E)$ changes linearly, and as can be seen from eq 4, to obtain an appreciable effect from the SPP field, $4\alpha\beta$ has to be small compared to μ^2. This means that the electron has to be transferred frequently between the HOMO and the LUMO before it escapes into the contacts at a rate proportional to β or before it leaks out through the LUMO at a rate proportional to α. Another observation about eq 4 is that $T(0)$ approaches 1 for $\mu \to 0$, underlining the role of the SPP.

Instead of the source−sink potentials, the contacts can also be accounted for within the more conventional Green function approach (see e.g., refs[23,24,32]), and we would like to stress that the source−sink potential approach gives results equivalent to the Green function approach as demonstrated in ref 33. To qualitatively confirm the mechanism of the molecular switch, we note that the transmission probability in the model discussed above [panel (a) of Figure 2] is proportional to[32] the local density of states on the HOMO site ($\rho_{\mathrm{HOMO}}(E)$). This density of states vanishes at the HOMO energy ($\rho_{\mathrm{HOMO}}(E = \epsilon_{\mathrm{HOMO}}) = 0$) as a consequence of the coupling of the HOMO to the localized LUMO, whose energy is shifted by $-\omega$ to coincide with the HOMO energy. This is the well-known Fano effect.[18,30,31]

The models introduced in this and the following section can be extended beyond the two-level (HOMO and LUMO) systems,[26] and the molecules employed in the devices can be represented by single-particle Hamiltonians such as the Hückel Hamiltonian. This prescription has been followed to obtain the transmission probability for the 1,3-divinylthioazulene-based device in Figure 1. The resulting $T(E)$ clearly shows the same features as the two-level model presented above.

3. SURFACE PLASMON POLARITON ABSORPTION AND CONVERSION INTO ELECTRONIC ENERGY (INELASTIC SPP−MOLECULE INTERACTION)

Another interesting mechanism that should be viable within the realm of dressed molecules connected to external contacts is depicted in panel (b) of Figure 2. Particularly noteworthy is the fact that the HOMO is coupled to the left and the LUMO to the right contact. Such a coupling can, for instance, be achieved with an azulene-based device depicted below the scheme. A comparison of the HOMO and LUMO in Figure 1 confirms that the orbital−contact coupling is indeed asymmetric. The Hamiltonian matrix for the mechanism of Figure 2 is[26]

$$\mathbf{H} = \begin{pmatrix} g - i\beta & \mu \\ \mu & -g + \dfrac{i(r+1)\beta}{1-r} + \omega \end{pmatrix} \tag{5}$$

In this matrix, the SSP potentials act on different energy levels and the SPP energy quantum ω again reduces the effective HOMO−LUMO energy gap. Following the steps leading to eq 3, we obtain $T(E)$. As the resulting expression is somewhat cumbersome, we focus on certain simplifications of it. At resonance, where $\omega = 2g$, this expression can be cast into a transparent form using the factorization approach[34]

$$T(E) = 1 - \left| \frac{(g - \sqrt{\mu^2 - \beta^2} - E)(g + \sqrt{\mu^2 - \beta^2} - E)}{(g - i\beta - \mu - E)(g - i\beta + \mu - E)} \right|^2 \tag{6}$$

The transmission probability maximizes if the numerator in the second term vanishes. This condition is satisfied for $E = g \pm \sqrt{\mu^2 - \beta^2}$. For $\mu^2 \geq \beta^2$, the maxima are on the real energy axis, one below and one above the LUMO energy ($\epsilon_{\mathrm{LUMO}} = g = 1$), and the transmission probability rises to 1. The largest possible separation between the maxima is given by the Rabi splitting ($2|\mu|$). For $\mu^2 < \beta^2$, the maxima shift into the complex plane, so that the maximum transmission probability for physical, that is, real energies, drops below 1. In this case, the dressed states are quenched through the strong coupling with the contacts. The function $T(E)$ obtained from eq 6 is depicted in Figure 5.

The described photoelectric cell converts the SPP energy into electronic energy and results in a nonvanishing conductance. In the absence of the molecule−SPP coupling, $T(E) = 0$ for all values of E.

Maybe the easiest experimental measurements of the conductance can be made at the Fermi energy [in our case, ($E_F = 0$)] and in the zero-voltage limit. In this limit, at resonance ($\omega = 2g$), the transmission probability simplifies to

DOI: 10.1021/acs.jpcc.8b05190
J. Phys. Chem. C 2018, 122, 20083−20089

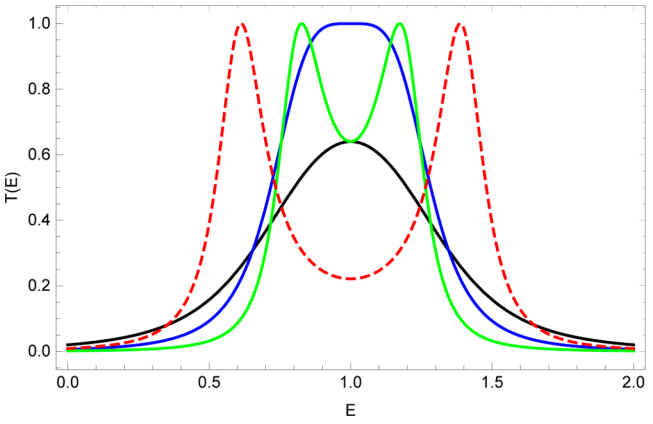

Figure 5. Transmission probability of a molecular photovoltaic cell converting SPP energy into electronic energy. The resonance condition, where the SPP energy equals the HOMO−LUMO gap, is satisfied. The HOMO−LUMO splitting is given by $2g$, with $g = 1$. The various curves are obtained upon variation of β = 0.1, 0.2, 0.4 corresponding to the green, blue, and black curves, respectively. In these cases, $\mu = 0.2$, whereas the red-dashed curve is obtained with μ = 0.4 and $\beta = 0.1$. In the absence of the molecule−SPP coupling, $T(E)$ vanishes for every value of E.

$$T(0) = \frac{4\beta^2\mu^2}{(\beta^2 + \mu^2)^2 + g^4 + 2g^2(\beta^2 - \mu^2)} \tag{7}$$

In Figure 6, $T(0)$ of eq 7 is plotted as a function of μ. The molecule−SPP system is considered at a resonance where $|\mu|$ is

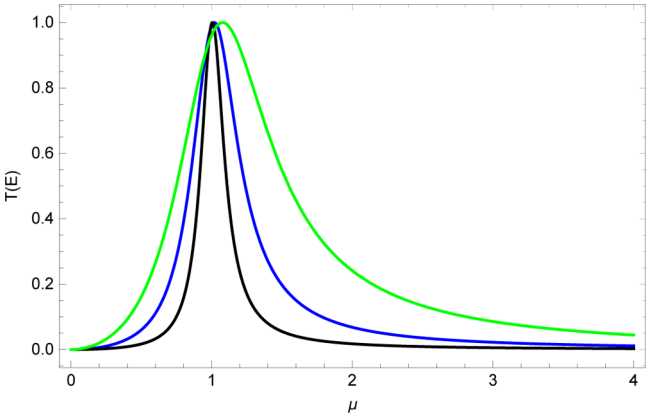

Figure 6. Transmission probability as a function of μ, which is half the Rabi frequency. The electron energy is equal to the Fermi energy and the system is at resonance. The black, blue, and green curves are obtained with β = 0.1, 0.2, and 0.4, respectively.

half the Rabi frequency. The maximum in $T(0)$ is obtained if the Rabi frequency is twice the value of g, where the Rabi splitting is such that there is a resonance at the Fermi energy. For small values of $|\mu|$, the transmission probability depends quadratically on μ, and for large values of $|\mu|$ the transmission probability approaches 0 as $1/\mu^2$; this is because the dressed states move further away from E_F, and this creates a barrier for electron transfer. Increasing β beyond the values used in Figure 6 eventually leads to a complete suppression of the transmission probability.

Until now, we considered the transmission probability as a function of energy. The total current I that is induced through the coupling of the molecule to the SPP is also of interest. To obtain I, we perform the integration over $T(E)$, that is

$$I = \frac{2e}{h}\int \mathrm{d}E T(E) = \frac{2e}{\hbar}\frac{\beta\mu^2}{\beta^2 + \mu^2} \tag{8}$$

This expression shows that I approaches a constant value as $|\mu|$ increases, that is, increasing the SPP field strength leads to photocurrent saturation. In the limit where $|\beta| \ll |\mu|$, we find

$$I \overset{|\beta|\ll|\mu|}{=} \frac{2e}{\hbar}\beta \tag{9}$$

that is, the current is simply proportional to β. In this limit, with increasing $|\mu|$, the two Rabi peaks move apart, but the integrated current remains constant. If, however, $|\beta| \gg |\mu|$, we obtain

$$I \overset{|\beta|\gg|\mu|}{=} \frac{2e}{\hbar}\frac{\mu^2}{\beta} \tag{10}$$

In this case, the total current is proportional the square of $\mu = -\mathbf{Ed}$ and thus to the square of the field strength, and hence to the energy density of the SPP.

An earlier suggestion of a device featuring light-induced currents through molecules is provided in ref 23, where also a quantized description of light is used. In a previous work[27] on photovoltaic cells, we developed and employed a scattering theory approach to describe molecular photocells. This approach, applied to the model system in panel (b) of Figure 2, yields results that are equivalent to the ones reported here.

4. DISCUSSION

Presently, strong SPP−molecule coupling is a research topic that is actively pursued, and the properties of the resulting mixed system of matter and light can be exploited, for instance, to realize new types of chemical reactions,[17] to yield new spectroscopic properties,[16] and also to fabricate new electronic devices.[18,19] The development of SPP-controlled electronic devices can be guided by simple, transparent device mechanisms. In the present work, we provide such device mechanisms together with the underlying theoretical model. This model, which we consider to be the simplest possible one, is an extension of the JC approach, and it can be employed to explore further device designs, beyond the ones discussed in this work.

The most appropriate molecule for building the proposed devices will depend on the experimental conditions; with 1,3-divinylthioazulene, we provide an example of how to satisfy the main requirement of the molecular switch−the LUMO must be isolated from the contacts. This can be achieved by connecting the molecule to the leads in such a way that the atoms which are attached to the contacts have a vanishing contribution to the LUMO. Note that the sulfur−ethylene bridges between the azulene molecule and the gold contacts are considered to be a part of the external leads. Similarly, azulene also provides an example of how to exploit the HOMO and LUMO structures to obtain a device with a highly asymmetrical orbital−contact coupling, resulting in a left-to-right current upon the absorption of the SPP quanta. The two devices discussed are the limiting cases that differ in the position of the Fermi energy with respect to the HOMO and LUMO energies; furthermore, the coupling of the HOMO and LUMO to the contacts is different. These limiting cases, and the admixtures of them, should be viable, given the wide range of contact materials, their geometries, and molecular structures available. Chemistry provides enormous flexibility for the design of molecules with a target set of

DOI: 10.1021/acs.jpcc.8b05190
J. Phys. Chem. C 2018, 122, 20083−20089

properties. The orbital energies can be shifted through various chemical modifications, and the nodal structure of the orbitals can be designed within wide boundaries.

The described devices involve SPPs which provide a strong field, which in turn results in large couplings between the ground and excited states (large $|\mu|$). The proposed switching mechanism is also operational if the fields are weak, such as in the case of ambient light. However, without the SPP field enhancement, $|\mu|$ will be several orders of magnitude smaller than a typical HOMO−LUMO splitting, and the conductance gap produced by the HOMO−LUMO coupling, which is proportional to $|\mu|$, might not be detectable. Similarly, the photovoltaic cell proposed above will also work without the SPP field enhancement. In this case, the total current through the cell is given by eq 10, which means that it is proportional to the square of the field strength and thus to the energy density of the electromagnetic field; this is the expected result.

AUTHOR INFORMATION

Corresponding Author

*E-mail: Matthias.Ernzerhof@UMontreal.ca.

ORCID

Matthias Ernzerhof: 0000-0001-5679-8902

Notes

The authors declare no competing financial interest.

ACKNOWLEDGMENTS

M.E. and A.G. acknowledge the financial support provided by NSERC. Furthermore, the authors are thankful for the technical assistance provided by Emil Grenier with the 3D graphics in Figure 1.

REFERENCES

(1) Dovzhenko, D. S.; Ryabchuk, S. V.; Rakovich, Y. P.; Nabiev, I. R. Light-matter Interaction in the Strong Coupling Regime: Configurations, Conditions, and Applications. *Nanoscale* **2018**, *10*, 3589−3605.

(2) Wang, T.; Nijhuis, C. A. Molecular Electronic Plasmonics. *Appl. Mater. Today* **2016**, *3*, 73−86.

(3) Ebbesen, T. W. Hybrid Light-Matter States in a Molecular and Material Science Perspective. *Acc. Chem. Res.* **2016**, *49*, 2403−2412.

(4) Xiang, D.; Wang, X.; Jia, C.; Lee, T.; Guo, X. Molecular-Scale Electronics: From Concept to Function. *Chem. Rev.* **2016**, *116*, 4318−4440.

(5) Bergfield, J. P.; Ratner, M. A. Forty Years of Molecular Electronics: Non-Equilibrium Heat and Charge Transport at the Nanoscale. *Phys. Status Solidi B* **2013**, *250*, 2249−2266.

(6) Ernzerhof, M.; Zhuang, M.; Rocheleau, P. Side-Chain Effects in Molecular Electronic Devices. *J. Chem. Phys.* **2005**, *123*, 134704.

(7) Ernzerhof, M.; Bahmann, H.; Goyer, F.; Zhuang, M.; Rocheleau, P. Electron Transmission through Aromatic Molecules. *J. Chem. Theory Comput.* **2006**, *2*, 1291−1297.

(8) Solomon, G. C.; Andrews, D. Q.; Van Duyne, R. P.; Ratner, M. A. Electron Transport through Conjugated Molecules: When the π System Only Tells Part of the Story. *ChemPhysChem* **2009**, *10*, 257−264.

(9) Tsuji, Y.; Estrada, E.; Movassagh, R.; Hoffmann, R. Quantum Interference, Graphs, Walks, and Polynomials. *Chem. Rev.* **2018**, *118*, 4887−4911.

(10) Solomon, G. C.; Andrews, D. Q.; Goldsmith, R. H.; Hansen, T.; Wasielewski, M. R.; Van Duyne, R. P.; Ratner, M. A. Quantum Interference in Acyclic Systems: Conductance of Cross-Conjugated Molecules. *J. Am. Chem. Soc.* **2008**, *130*, 17301−17308.

(11) Fracasso, D.; Valkenier, H.; Hummelen, J. C.; Solomon, G. C.; Chiechi, R. C. Evidence for Quantum Interference in SAMs of Arylethynylene Thiolates in Tunneling Junctions with Eutectic Ga-In (EGaIn) Top-Contacts. *J. Am. Chem. Soc.* **2011**, *133*, 9556−9563.

(12) Guédon, C. M.; Valkenier, H.; Markussen, T.; Thygesen, K. S.; Hummelen, J. C.; van der Molen, S. J. Observation of Quantum Interference in Molecular Charge Transport. *Nat. Nanotechnol.* **2012**, *7*, 305−309.

(13) Darwish, N.; Díez-Pérez, I.; Da Silva, P.; Tao, N.; Gooding, J. J.; Paddon-Row, M. N. Observation of Electrochemically Controlled Quantum Interference in a Single Anthraquinone-Based Norbornylogous Bridge Molecule. *Angew. Chem., Int. Ed.* **2012**, *51*, 3203−3206.

(14) Ballmann, S.; Härtle, R.; Coto, P. B.; Elbing, M.; Mayor, M.; Bryce, M. R.; Thoss, M.; Weber, H. B. Experimental Evidence for Quantum Interference and Vibrationally Induced Decoherence in Single-Molecule Junctions. *Phys. Rev. Lett.* **2012**, *109*, 056801.

(15) Rabache, V.; Chaste, J.; Petit, P.; Della Rocca, M. L.; Martin, P.; Lacroix, J.-C.; McCreery, R. L.; Lafarge, P. Direct Observation of Large Quantum Interference Effect in Anthraquinone Solid-State Junctions. *J. Am. Chem. Soc.* **2013**, *135*, 10218−10221.

(16) Chikkaraddy, R.; de Nijs, B.; Benz, F.; Barrow, S. J.; Scherman, O. A.; Rosta, E.; Demetriadou, A.; Fox, P.; Hess, O.; Baumberg, J. J. Single-molecule Strong Coupling at Room Temperature in Plasmonic Nanocavities. *Nature* **2016**, *535*, 127−130.

(17) de Nijs, B.; Benz, F.; Barrow, S. J.; Sigle, D. O.; Chikkaraddy, R.; Palma, A.; Carnegie, C.; Kamp, M.; Sundararaman, R.; Narang, P.; Scherman, O. A.; Baumberg, J. J. Plasmonic Tunnel Junctions for Single-molecule Redox Chemistry. *Nat. Commun.* **2017**, *8*, 994.

(18) Zhang, Y.; Meng, Q.-S.; Zhang, L.; Luo, Y.; Yu, Y.-J.; Yang, B.; Zhang, Y.; Esteban, R.; Aizpurua, J.; Luo, Y.; Yang, J.-L.; Dong, Z.-C.; Hou, J. G. Sub-Nanometre Control of The Coherent Interaction Between a Single Molecule and a Plasmonic Nanocavity. *Nat. Commun.* **2017**, *8*, 15225.

(19) Vadai, M.; Nachman, N.; Ben-Zion, M.; Bürkle, M.; Pauly, F.; Cuevas, J. C.; Selzer, Y. Plasmon-Induced Conductance Enhancement in Single-Molecule Junctions. *J. Phys. Chem. Lett.* **2013**, *4*, 2811−2816.

(20) Flick, J.; Ruggenthaler, M.; Appel, H.; Rubio, A. Atoms and Molecules in Cavities, from Weak to Strong Coupling in Quantum-electrodynamics (QED) Chemistry. *Proc. Natl. Acad. Sci. U.S.A.* **2017**, *114*, 3026−3034.

(21) White, A. J.; Fainberg, B. D.; Galperin, M. Collective Plasmon-Molecule Excitations in Nanojunctions: Quantum Consideration. *J. Phys. Chem. Lett.* **2012**, *3*, 2738−2743.

(22) Galperin, M. Photonics and Spectroscopy in Nanojunctions: a Theoretical Insight. *Chem. Soc. Rev.* **2017**, *46*, 4000−4019.

(23) Galperin, M.; Nitzan, A. Current-Induced Light Emission and Light-Induced Current in Molecular-Tunneling Junctions. *Phys. Rev. Lett.* **2005**, *95*, 206802.

(24) Galperin, M.; Nitzan, A. Molecular Optoelectronics: The Interaction of Molecular Conduction Junctions with Light. *Phys. Chem. Chem. Phys.* **2012**, *14*, 9421−9438.

(25) Jaynes, E. T.; Cummings, F. W. Comparison of Quantum and Semiclassical Radiation Theories with Application to the Beam Maser. *Proc. IEEE* **1963**, *51*, 89−109.

(26) Ernzerhof, M.; Bélanger, M.-A.; Mayou, D.; Nemati Aram, T. Simple Model of a Coherent Molecular Photocell. *J. Chem. Phys.* **2016**, *144*, 134102.

(27) Nemati Aram, T.; Anghel-Vasilescu, P.; Asgari, A.; Ernzerhof, M.; Mayou, D. Modeling of Molecular Photocells: Application to Two-level Photovoltaic System with Electron-hole Interaction. *J. Chem. Phys.* **2016**, *145*, 124116.

(28) Nemati Aram, T.; Ernzerhof, M.; Asgari, A.; Mayou, D. The Impact of Long-range Electron-hole Interaction on the Charge Separation Yield of Molecular Photocells. *J. Chem. Phys.* **2017**, *146*, 034103.

(29) Goyer, F.; Ernzerhof, M.; Zhuang, M. Source and Sink Potentials for the Description of Open Systems with a Stationary Current Passing Through. *J. Chem. Phys.* **2007**, *126*, 144104.

(30) Miroshnichenko, A. E.; Flach, S.; Kivshar, Y. S. Fano Resonances in Nanoscale Structures. *Rev. Mod. Phys.* **2010**, *82*, 2257−2298.

DOI: 10.1021/acs.jpcc.8b05190
J. Phys. Chem. C 2018, 122, 20083−20089

(31) Liu, Z.; Li, J.; Liu, Z.; Li, W.; Li, J.; Gu, C.; Li, Z.-Y. Fano Resonance Rabi Splitting of Surface Plasmons. *Sci. Rep.* **2017**, *7*, 8010.
(32) Meir, Y.; Wingreen, N. S.; Lee, P. A. Transport Through a Strongly Interacting Electron System: Theory of Periodic Conductance Oscillations. *Phys. Rev. Lett.* **1991**, *66*, 3048−3051.
(33) Fowler, P. W.; Pickup, B. T.; Todorova, T. Z. A Graph-Theoretical Model for Ballistic Conduction in Single-Molecule Conductors. *Pure Appl. Chem.* **2011**, *83*, 1515−1528.
(34) Ernzerhof, M. A Simple Model of Molecular Electronic Devices and Its Analytical Solution. *J. Chem. Phys.* **2007**, *127*, 204709.

DOI: 10.1021/acs.jpcc.8b05190
J. Phys. Chem. C 2018, 122, 20083−20089